Solid State Synthesis, Crystal Structure, Decomposition Reactions, and Optical Nonlinearity of a Twin-Nest-Shaped Cluster Compound, $[Et_4N]_4[Mo_2O_2S_6Cu_6I_6]$

Hongwei Hou,[†] Deliang Long,[†] Xinquan Xin,[†] Xiaoxing Huang,[‡] Beisheng Kang,[‡] Ping Ge,[§] Wei Ji,[§] and Shu Shi*[,§]

State Key Laboratory of Coordination Chemistry, Department of Chemistry, Nanjing University, Nanjing 210093, China, State Key Laboratory of Structural Chemistry, Fujian Institute of Research on Structure of Matter, Chinese Academy of Science, Fuzhou 350002, China, and Department of Chemical Engineering and Department of Physics, National University of Singapore, Singapore 0511

Received August 3, 1995[⊗]

The reaction of $(NH_4)_2[MoO_2S_2]$, CuI, and Et_4NI in solid state produces a twin-nest-shaped cluster compound $[Et_4N]_4[Mo_2O_2S_6Cu_6I_6]$. The cluster anion consists of two nest-shaped fragments interconnected through a four-membered $Cu(I)_2Cu$ ring. The structure of the cluster has been characterized by X-ray diffraction: monoclinic, space group $C2/c$, $a = 24.680(1)$ Å, $b = 21.328(5)$ Å, $c = 13.638(4)$ Å, $\beta = 114.51(3)°$, $V = 6532(4)$ Å^3, $Z = 4$, $R = 0.043$, $R_w = 0.054$. The cluster easily decomposes into two halves when treated with ligands such as py or PPh_3. The cluster also exhibits both strong nonlinear optical absorption and optical self-defocusing effect (effective $\alpha_2 = 4 \times 10^{-10}$ m W^{-1}, $n_2 = -6 \times 10^{-17}$ m^2 W^{-1}, when measured with a 2×10^{-3} M acetonitrile solution).

Introduction

The tetrathiometalates MS_4^{2-} (M = Mo, W) have shown to be able to act as multidentate ligands with a variety of transition metal ions.[1] They have been used extensively as starting materials in synthesizing Mo(W) containing inorganic clusters[2,3] and in catalytic studies.[4,5] Recently, studies on these clusters have been expanded to include their nonlinear optical (NLO) properties. Traditionally, NLO research has been largely focused on semiconductors, conjugated polymers, and discrete organic molecules.[6,7] In our search for better NLO materials, we have undertaken a series of studies on structure and NLO properties of Mo(W)−S(O)−Cu(Ag) clusters.[8−13] Recently, we discovered that butterfly shaped clusters $[MOS_3Cu_2(PPh_3)_x]$ (M = Mo, W; $x = 3$, 4)[12] exhibit strong third-order NLO refractive effect (self-focusing), but their nest-shaped derivatives, $(n\text{-}Bu_4N)_2[MoOS_3Cu_3BrCl_2]$ and $(n\text{-}Bu_4N)_2[MoOS_3Cu_3(NCS)_3]$, behave quite differently. The self-focusing effect observed in the family of butterfly-shaped clusters is replaced by a self-defocusing effect in the family of the nest-shaped clusters.[10,11] Here, we report our study on an example of a twin-nest-shaped cluster, $[Et_4N]_4[Mo_2O_2S_6Cu_6I_6]$. A twin-nest-shaped cluster may be regarded as a dimer of two nest-shaped units. We discuss solid state synthesis, structure, and electronic spectrum of the cluster along with its decomposition reactions caused by PPh_3 and py. We also compare its third-order NLO absorptive and refractive properties with those of other related clusters and compounds.

Experimental Section

The compound $(NH_4)_2MoO_2S_2$ was prepared as described in the literature.[14] The other chemicals were purchased as AR reagents and used without further purification.

Infrared spectra were recorded with a Fourier transform Nicolet FT-170SX spectrophotometer with pressed KBr pellets. The electronic spectrum was taken on a Shimadzu UV-240 spectrophotometer. Elemental analysis of carbon, hydrogen, and nitrogen were performed on a PE 240C elemental analyzer.

Preparation of $[Et_4N]_4[Mo_2O_2S_6Cu_6I_6]$. A well-ground mixture of $(NH_4)_2MoO_2S_2$ (0.23 g, 1 mmol), CuI (0.38 g, 2 mmol), and Et_4NI (0.52 g, 2 mmol) was put into a reaction tube and heated at 92 °C for 10 h in a pure nitrogen atmosphere. Extraction of the brown solid product with CH_2Cl_2 (20 mL) and dropwise addition of 2-propanol (10 mL) to the top of the filtration solutions produced a white precipitate. Filtering the deep red solution, we obtained black crystals (0.24 g) several days later. The compound is insoluble either in ether or in ethanol but soluble in CH_2Cl_2, THF, CH_3CN, and DMF. It shows characteristic infrared absorption peaks at 901 cm^{-1}, ν(Mo−O$_t$), and 447 cm^{-1}, ν(Mo−S$_{br}$). Anal. Calcd for $C_{32}H_{80}Cu_6I_6Mo_2N_4O_2S_6$: C, 18.47; H, 3.84; N, 2.69. Found: C, 18.62; H, 3.76; N, 2.70.

Reaction with py. A 0.10 g sample of $[Et_4N]_4[Mo_2O_2S_6Cu_6I_6]$ was added to py (20 mL). Stirring for 2 h and filtering, we obtained a clear deep red solution. Dropwise addition of 2-propanol (10 mL) to the top of the solution resulted in the formation of black crystals (0.06 g) after the solution was allowed to stand for 1 week. The compound is slightly soluble in CH_3CN, THF, and DMF and was identified as

* To whom correspondence should be addressed.
[†] Nanjing University.
[‡] Chinese Academy of Science.
[§] National University of Singapore.
[⊗] Abstract published in *Advance ACS Abstracts,* July 1, 1996.

(1) Muller, A.; Diemann, E.; Jostes, R.; Bogge, H. *Angew. Chem. Int. Ed. Engl.* **1981**, *20*, 934.
(2) Lang, J. P.; Xin, X. Q. *J. Solid State Chem.* **1994**, *108*, 118.
(3) Hou, H. W.; Lang, J. P.; Li, J. G.; Xin, X. Q. *Chin. J. Inorg. Chem.* **1994**, *10*, 218.
(4) Holm, R. H. *Chem. Soc. Rev.* **1981**, *10*, 455.
(5) Bremner, I.; Mills, C. F.; Young, B. W. *J. Inorg. Biochem.* **1982**, *16*, 109.
(6) Chemla, D. S.; Zyss, J., Eds. *Nonlinear Optical Properties of Organic Molecules and Crystals*; Academic: Orlando, FL, 1987.
(7) Huang, H., Ed. *Optical Nonlinearities and Instabilities in Semiconductors*; Academic: Boston, MA, 1988.
(8) Shi, S.; Ji, W.; Tang, S. H.; Lang, J. P.; Xin, X. Q. *J. Am. Chem. Soc.* **1994**, *116*, 3615.
(9) Shi, S.; Ji, W.; Lang, J. P.; Xin, X. Q. *J. Phys. Chem.* **1994**, *98*, 3570.
(10) Shi, S.; Ji, W.; Xie, W.; Chong, T. C.; Zeng, H. C.; Lang, J. P.; Xin, X. Q. *Mater. Chem. Phys.* **1995**, *39*, 298.
(11) Hou, H. W.; Ye, X. R.; Xin, X. Q.; Liu, J.; Chen, M. Q.; Shi, S. *Chem. Mater.* **1995**, *7*, 472.
(12) Shi, S.; Hou, H. W.; Xin, X. Q. *J. Phys. Chem.* **1995**, *99*, 4050.
(13) Hou, H. W.; Xin, X. Q.; Liu, J.; Chen, M. Q.; Shi, S. *J. Chem. Soc., Dalton Trans.* **1994**, 3211.
(14) McDonald, J. W.; Frieson, G. D.; Rosenhein, C. D.; Newton, W. E. *Inorg. Chim. Acta* **1983**, *72*, 205.

S0020-1669(95)00991-8 CCC: $12.00

Table 1. Crystal Parameters for the Cluster $[Et_4N]_4[Mo_2O_2S_6Cu_6I_6]$[a]

chem formula: $C_{32}H_{80}Cu_6I_6N_4Mo_2O_2S_6$	space group: *C*2/*c*
$a = 24.680(1)$ Å	$T = 23$ °C
$b = 21.328(5)$ Å	$\lambda = 0.71069$ Å (MoKα)
$c = 13.638(4)$ Å	$\rho_{calc} = 2.11$ g/cm^3
$\beta = 114.51(3)$	μ(Mo Kα) = 53.05 cm^{-1}
$V = 6532(4)$ Å^3	$R = 0.043$
$Z = 4$	$R_w = 0.054$
fw 2079.95	

[a] Definitions: $R = \sum|F_o| - |F_c| /\sum|F_o|$; $R_w = [\sum w(|F_o| - |F_c|)^2/\sum wF_o2]^{1/2}$; $w = 1/\sigma^2(F_o) = 4F_o^2/\sigma^2(F_o^2)$; $\sigma^2(F_o^2) = [S^2(C + R^2B) + (pF_o^2)^2]/Lp^2$; S = scan rate; C = total integrated peak count; R = ratio of scan time to background counting time; B = total background counting; p = p-factor; Lp = Lorentz−polarization factor;

Table 2. Positional Parameters and *B*(eq) Values for $[Et_4N]_4[Mo_2O_2S_6Cu_6I_6]$

atom	*x*	*y*	*z*	*B*(eq) (Å^2)
Mo	0.24869(5)	0.21500(6)	0.30463(1)	4.22(5)
I(1)	0.34567(4)	0.26290(5)	0.05355(7)	5.65(4)
I(2)	0.08514(4)	0.37898(4)	0.15799(8)	5.38(8)
I(3)	0.12285(6)	0.03608(5)	0.0884(2)	11.38(8)
Cu(1)	0.27290(9)	0.23893(8)	0.1342(2)	5.93(8)
Cu(2)	0.16094(7)	0.29565(7)	0.2092(1)	5.08(7)
Cu(3)	0.17977(8)	0.12891(8)	0.1755(2)	6.09(8)
S(1)	0.2570(1)	0.3108(2)	0.2438(3)	4.7(1)
S(2)	0.2765(2)	0.1435(2)	0.2134(3)	5.3(2)
S(3)	0.1506(2)	0.1990(2)	0.2659(3)	5.2(2)
O	0.2923(4)	0.2069(5)	0.4392(8)	7.4(5)
N(1)	0.3174(6)	0.0033(5)	0.5160(1)	5.1(5)
N(2)	0.0448(5)	0.1910(5)	0.5223(8)	4.9(5)

$[MoOS_3Cu_3I(py)_5]$ by IR spectra (ν(Mo−O$_t$), 914 cm^{-1}; ν(Mo-O$_{br}$), 441 cm^{-1}) and elemental analysis.[15]

Reaction with PPh_3. A solution of 0.05 g of $[Et_4N]_4[Mo_2O_2S_6Cu_6I_6]$ in CH_3CN (10 mL) was added to a solution of 0.02 g of PPh_3 in CH_3CN (10 mL). Within 1 day at room temperature, deep red crystals (0.02 g) were obtained. The compound is insoluble in CH_3CN or THF but slightly soluble in DMF. It was identified as $[MoOS_3Cu_3I(PPh_3)_3]$ by IR spectra (ν(Mo−O$_t$), 923 cm^{-1}; ν(Mo−S$_{br}$), 445 cm^{-1}) and elemental analysis.[16]

Crystal Structure and Determination and Refinement. A suitable crystal was mounted in random orientation on a glass fiber. Data were collected on a Rigaku AFC5R diffractometer using Mo Kα radiation at 296 K. The crystallographic data and details concerning the intensity are summarized in Table 1. The data were corrected for Lorentz and polarization factors and for absorption by using empirical scan data.

The structure was initially solved by heavy atom methods which revealed the position of the Mo and Cu atoms. The remaining non-hydrogen atoms were located in successive difference Fourier maps. The structure was refined by full-matrix least-squares method to final $R = 0.043$ and $R_w = 0.054$. All calculations were carried out on MICRO-VAXII with TEXSAN program package.[17] The atomic coordinates and thermal parameters are listed in Table 2.

Optical Measurements. An acetonitrile solution of 2×10^{-3} M of the title compound was placed in a 1-mm quartz cuvette for optical measurements. Their nonlinear absorption and nonlinear refraction were measured with a linearly polarized laser light ($\lambda = 532$ nm; pulse width = 7 ns) generated from a Q-switched and frequency-doubled Nd-YAG laser. The spatial profiles of the optical pulses were nearly Gaussian. The laser beam was focused with a 25-cm focal-length focusing mirror. The radius of the beam waist was measured to be 30 ± 5 μm (half-width at 1/e^2 maximum). The incident and transmitted pulse energy were measured simultaneously by two Laser Precision detectors (RjP-735 energy probes) which were linked to a computer by an IEEE interface. The nonlinear optical properties of the samples were manifested by moving the samples along the axis of incident beam (Z-direction) with respect to the focal points.[18] An aperture of 0.5 mm radius was placed in front of a detector that was positioned behind the sample to assist the measurement of self-defocusing effect of the sample.

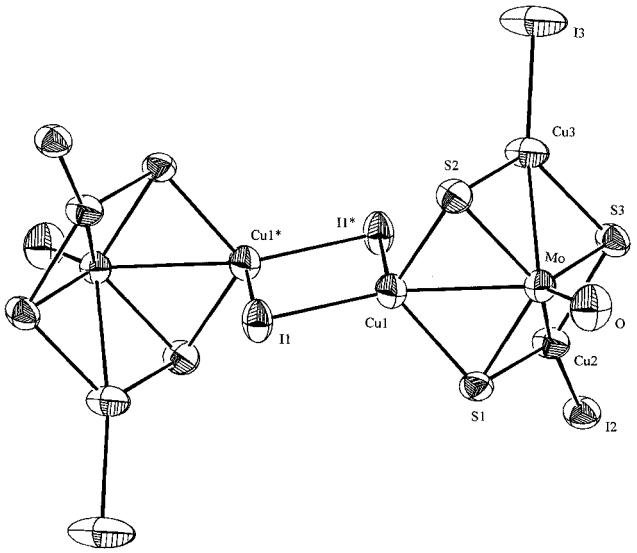

Figure 1. ORTEP diagram of the anionic cluster $[Mo_2O_2S_6Cu_6I_6]^{4-}$.

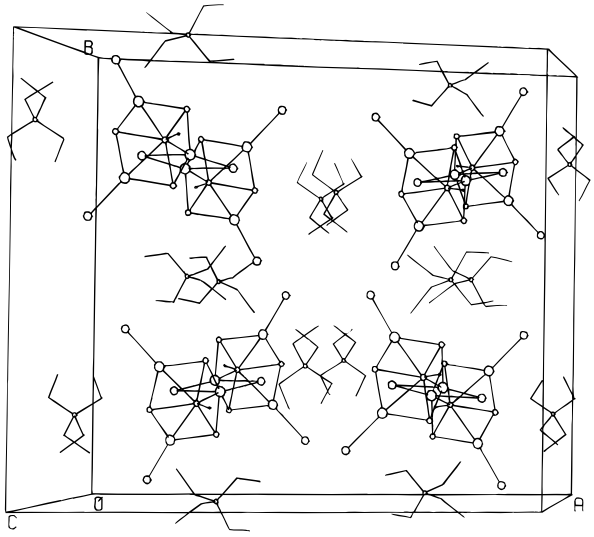

Figure 2. Arrangement of the Et_4N^+ cations and the $[Mo_2O_2S_6Cu_6I_6]^{4-}$ anions in a cell.

Results and Discussion

Structure of $[Et_4N]_4[Mo_2O_2S_6Cu_6I_6]$. The cluster ion consists of two nest-shaped $[MoOS_3Cu_3I_3]^{2-}$ fragments interconnected through a four-membered $Cu(I)_2Cu$ ring. The ORTEP diagram of the $[Mo_2O_2S_6Cu_6I_6]^{4-}$ anion and the crystal packing scheme of the compound are shown in Figures 1 and 2, respectively. In each of the fragments, one I atom is attached to each of the three Cu atoms, and the terminal O atom is attached to the Mo atom. The Mo−O distance of 1.700(1) Å is typical for an Mo=O double bond. The three Mo−S bonds, 2.255(4)−2.274(4) Å, fall in the range of a typical Mo−S single bond. The O−Mo−S bond angles range from 109.4(4) to 112.3(4)°, whereas the three S−Mo−S angles range from 107.4-(1) to 107.6(1)°. Clearly, the Mo atom has basically retained the pseudotetrahedral geometry of the free $[MoOS_3]^{2-}$ anion. Table 3 compiles selected bond lengths and bond angles.

(15) Hou, H. W.; Xin, X. Q.; Lu, S. F.; Huang, X. Y.; Wu, Q. J. *J. Coord. Chem.*, in press.
(16) Hou, H. W.; Xin, X. Q.; Shi, S. To be submitted for publication.
(17) TEXSAN-TEXRAY Structure Analysis Package. Molecular Structure Corp., 1985.
(18) Sheik-Bahae, M.; Said, A. A.; Wei, T. H.; Hagan, D. J.; Van Stryland, E. W. *IEEE J. Quantum Electron.* **1990**, 26, 760.

Table 3. Selected Bond Lengths (Å) and Bond Angles (deg)

I(1)−Cu(1)	2.517(2)	I(1)−Cu(1a)	2.984(3)	I(2)−Cu(2)	2.462(2)
I(3)−Cu(3)	2.433(2)	Mo−O	1.69(1)	Mo−S(1)	2.256(4)
Mo−S(2)	2.264(4)	Mo−S(3)	2.274(4)	Mo−Cu(3)	2.633(2)
Mo−Cu(2)	2.650(2)	Mo−Cu(1)	2.700(2)	S(1)−Cu(1)	2.285(4)
S(2)−Cu(1)	2.288(4)	S(1)−Cu(2)	2.241(4)	S(3)−Cu(2)	2.252(4)
S(3)−Cu(3)	2.239(4)	S(2)−Cu(3)	2.245(4)		
O−Mo−S(1)	112.4(4)	O−Mo−S(2)	109.0(4)	O−Mo−S(3)	112.6(4)
O−Mo−Cu(3)	126.9(4)	O−Mo−Cu(2)	128.8(4)	O−Mo−Cu(1)	132.8(3)
S(1)−Mo−S(2)	107.6(1)	S(1)−Mo−S(3)	107.4(1)	S(2)−Mo−S(3)	107.6(2)
S(1)−Cu(1)−S(2)	105.8(1)	S(1)−Cu(1)−I(1)	119.8(1)	S(2)−Cu(1)−I(1)	119.5(1)
S(1)−Cu(2)−I(2)	124.7(1)	I(3)−Cu(3)−Mo	168.1(1)	I(1)−Cu(1)−Mo	150.9(1)
Cu(1)−I(1)−Cu(1a)	75.4(1)	I(1a)−Cu(1)−I(1)	104.6(1)		

Scheme 1

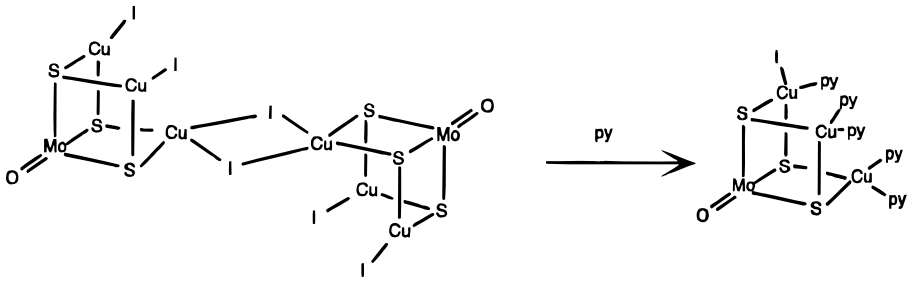

In $[Mo_2O_2S_6Cu_6I_6]^{4-}$, two distinctly different coordination geometries of copper coexist. The Cu(2) and Cu(3) atoms adopt trigonal planar geometry (coordinated by two S and one I atom), while Cu(1) atom adopts distorted tetrahedral geometry (coordinated by two S and two I atoms). Atoms Cu(2) and Cu(3) are roughly in planes containing either Mo, S(1), S(3), I(2) or Mo, S(2), S(3), I(3). Certain extent of π-bonding is expected to form over these planes. This is consistent with the observed shorter Mo−Cu(2) distance (2.652(2) Å) and Mo−Cu(3) distance (2.633(2) Å) as compared to the Mo−Cu(1) distance of 2.699(2) Å. In similar nest-shaped clusters $[(n\text{-}Bu_4)N]_2[MoOS_3(CuSCN)_3]$[19] and $[(n\text{-}Bu_4)N]_2[MoOS_3Cu_3BrCl_2]$,[11] trigonal planar coordination geometry is adopted by all of three Cu atoms, and relatively short Mo−Cu distances (2.650(2), 2.652(2), and 2.638(2) Å in $[(n\text{-}Bu_4)N]_2[MoOS_3(CuSCN)_3]$ and 2.621(1), 2.628(1), and 2.638(1) Å in $[(n\text{-}Bu_4)N]_2[MoOS_3Cu_3BrCl_2]$) are observed.

Reactions. In Mo(W)−Cu(Ag)−S clusters, terminal ligands such as Cl^-, Br^-, and I^- have been proposed to be loosely bound and can be substituted by strong ligands such as PPh_3 and py to produce desired derivatives. Clusters of high nuclearity may decompose into clusters of lower nuclearity in the presence of extra ligands. The reactions usually start from a ligand substitution at an M′−S or M′−X (M′ = Cu, Ag; X = Cl, Br, I) unit.

The reaction of the nest-shaped cluster $[Et_4N]_4[Mo_2O_2S_6Cu_6I_6]$ with py is illustrated in Scheme 1. The substitution of the terminal I^- by a py ligand is obviously accompanied by the breakage of the four-membered $Cu(I_2)Cu$ ring. Only one I^- remains attached as terminal ligand to a Cu atom in the nest-shaped product, $[MoOS_3Cu_3I(py)_5]$.

When the compound $[Et_4N]_4[Mo_2O_2S_6Cu_6I_6]$ is reacted with PPh_3, a cubane-like cluster $[MoOS_3Cu_3I(PPh_3)_3]$ is formed (Scheme 2). Apparently, the formation of the Cu−P bonds has enhanced the ability for the I atom to assume a μ_3-position. Structures of products in both Scheme 1 and Scheme 2 are known.[20]

Linear and Nonlinear Optical Properties. The cluster $[Et_4N]_4[Mo_2O_2S_6Cu_6I_6]$ shows linear and nonlinear optical properties similar to the nest-shaped clusters $[(n\text{-}Bu)_4N]_2[MoOS_3Cu_3BrCl_2]$ and $[(n\text{-}Bu_4)N]_2[MoOS_3Cu_3(NCS)_3]$. The electronic spectrum of the title compound is shown in Figure 3. Absorption peaks were observed at 409 and 289 nm which are similar to the absorption peaks of simple nest-shaped cluster $[(n\text{-}Bu)_4N]_2[MoOS_3Cu_3BrCl_2]$ at 408 and 286 nm.[11] Both strong NLO absorption and NLO refraction were observed with $[Et_4N]_4[Mo_2O_2S_6Cu_6I_6]$.

The NLO property of $[Et_4N]_4[Mo_2O_2S_6Cu_6I_6]$ was revealed by using a *Z*-scan technique.[18] Its nonlinear absorptive property is depicted by the open circles in Figure 4 while its nonlinear refractive property is depicted by the filled circles in the figure. The solid curves in the figure are generated theoretically using eqs 1 and 2.

$$T(z) = \frac{1}{\sqrt{\pi}q(z)}\int_{-\infty}^{+\infty}\ln[1 + q(z)]e^{-\tau^2}\,d\tau \qquad (1)$$

$$T(z,s) = \frac{\int_{-\infty}^{+\infty}P_T(t)\,dt}{s\int_{-\infty}^{+\infty}P_i(t)\,dt} \qquad (2)$$

Equation 1 describes the typical and pure absorptive behavior of a hypothetical third-order NLO process. The function $q(z)$ is defined by $q(z) = \int_0^\infty\int_0^\infty \alpha_2 I_i(r,t,z)L_{eff}r\,dr\,dt$ where α_2 is the nonlinear absorption coefficient of the cluster at 532 nm. $L_{eff} = [1 - \exp(-\alpha_0 L)]/\alpha_0$ with α_0 being the linear absorption coefficient of the cluster and L being the sample thickness (1 mm in this study). $I_i(r,t,z) = \{I_0/[1 + (z/z_0)^2]\}\exp[-2(r/\omega_0)^2 - (t/t_0)^2]$ is the incident irradiance with $z_0 = \pi\omega_0^2/\lambda$ and $\omega^2 = \omega_0^2[1 + (z/z_0)^2]$, where I_0 is the peak irradiance at focus, r is the radial coordinate, t is the time, t_0 is the pulse width, ω_0 is the spot radius of the laser beam at focus, and λ is the wavelength of the laser. Equation 2 describes the transmittance change detected behind a pinhole when both NLO absorptive and NLO refractive properties are considered. $P_i(t) = (1/2)I_0\pi\omega_0^2\exp[-(t/t_0)^2]$ and $P_T(z,t) = \epsilon_0 c n_0 \pi \int_0^{r_a}|E_a(r,t,z)|^2 r\,dr$ where ϵ_0 and c are the permittivity and speed of light

(19) Lang, J. P.; Bao, S. A.; Zhu, H. Z.; Xin, X. Q.; Cai, J. H.; Weng, L. H.; Wu, Y. H.; Kang, B. S. *Chin. Gaodeng Xuexiao Huaxue Xuebao* **1992**, *13*, 889.
(20) Hou, H. W. Ph.D. Thesis, Nanjing University, Nanjing, China, 1995.

Scheme 2

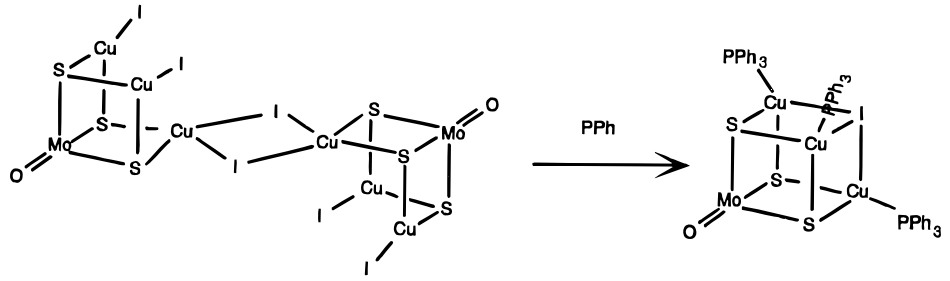

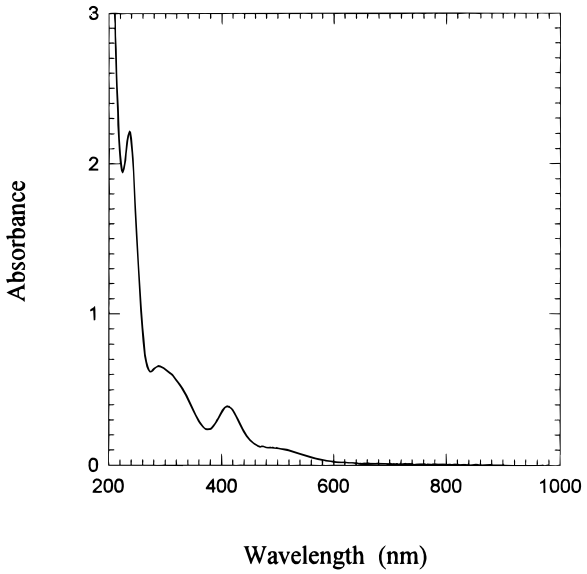

Figure 3. Electronic spectrum of $[Et_4N]_4[Mo_2O_2S_6Cu_6I_6]$ in CH_3CN. The concentration of the compound is 2×10^{-3} M. The optical path used for the measurement is 1 mm.

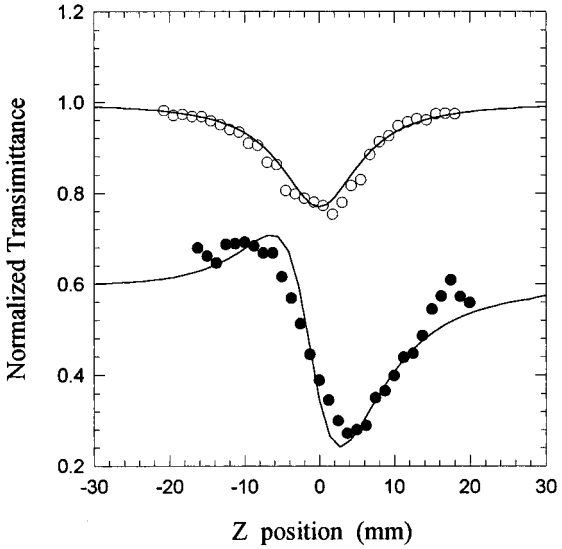

Figure 4. *Z*-scan data. Key: open circles, observed under an open aperture configuration; upper solid curve, theoretical curve based on eq 1; filled circles, *Z*-scan data observed under a closed aperture configuration divided by those obtained under the open aperture configuration to filter out the influence of NLO absorption; lower solid curve, a theoretical curve obtained from eq. 2 by setting $\alpha_2 \rightarrow 0$. Conditions: incident energy, 32 μJ; cluster concentration, 2×10^{-3} M.

in vacuum and n_0 is the linear refractive index of the sample. At the aperture, the electric component of the optical field is given by $E_a(r,t,z) = \{[2\pi/i\lambda(l - z)] \exp[i\pi r^2/\lambda(l - z)]\} \int_0^\infty \{r'E(r',t,z)J_0(2\pi r'r/\lambda(l - z))\exp[i\pi r'^2/\lambda(l - z)]\}\, dr'$ in which l is the distance between the aperture and the focus, $E(r',t,z) = [2(I(r',t,z)/\epsilon_0 c n_0)^{1/2}] \exp\{(kn_2/\alpha_2) \ln[1 + q(r',t,z)]\}$ and $J_0(x)$ is the zeroth-order Bessel's function. $S = 1 - \exp[-2(r_a/\omega_a)^2]$ is the linear aperture transmittance.

It is obvious that the theoretical curves qualitatively reproduce well the general pattern of the observed experimental data. This fact suggests an effectively third-order characteristic for the experimentally detected NLO effects (note that the NLO measurements were conducted in a 2×10^{-3} M acetonitrile solution of $[Et_4N]_4[Mo_2O_2S_6Cu_6I_6]$, where the presence of a macroscopic inversion center renders all of the even-order NLO effect to zero). The effective α_2- and n_2-values[21] used for the theoretical curves are 4×10^{-10} m W^{-1} and -6×10^{-17} m^2 W^{-1}, respectively. A control experiment shows that neither photodamage of the quartz cell containing the solution of $[Et_4N]_4[Mo_2O_2S_6Cu_6I_6]$ nor bubble formation in the solution due to local heating occurs to any detectable extent under the condition used in this study. To put the optical nonlinearity of cluster $[Et_4N]_4[Mo_2O_2S_6Cu_6I_6]$ in a proper perspective with reference to other known third-order NLO materials, these effective α_2- and n_2-values are listed in Table 4 along with the reported α_2- and n_2-values of related inorganic clusters and a few best performing semiconductors and organic polymers. Most of the well performing third-order NLO materials reported in the literature are solid materials (e.g. semiconductors and conjugated polymers). These are neat materials. One notices from Table 4 that impressive optical nonlinearity is achieved with much diluted inorganic clusters. Since both α_2- and n_2-values are expected to be proportional to the concentration of the NLO chromophore, much superior NLO performance can be expected if the solubilities of the inorganic clusters can be improved significantly. Currently the upper limits of the concentrations of these clusters, which are close to the concentration quoted in Table 4, are set by their low solubility in common organic solvents.

It is noted that there exists a certain discrepancy between the theoretical curve and the experimental data when both NLO absorption and NLO refraction are involved. Apparently, factors other than pure third-order NLO effects are also contributing.

Two important considerations that went into the design and synthesis of the nest-shaped and the twin-nest-shaped clusters are the following: (1) The cluster anions (the NLO chromophores) do not contain any A−H (A is a C, N, or O atom) bonds. (The organic countercations can in principle be easily replaced with inorganic cations via an ion exchange.) It is well recognized that the A−H overtone absorption of most organic NLO chromophores in the near-infrared region may result in significant loss in the intensity of the optical signals propagating through the NLO media. The absence of the A−H bonds in these inorganic clusters therefore presents a potentially very

(21) Both excited state absorption and two-photon absorption can be responsible for the measured NLO effects. The NLO parameters derived in this paper should be considered only as effective parameters because the existing experimental data are insufficient to identify the relative contributions of these two mechanisms.

Table 4. Optical Parameters of Selected NLO Chromophores

compound	concn (M)	λ (nm)	α_2 (m W^{-1})	n_2 (m^2 W^{-1})	ref
GaInAs	neat	1500		4.5×10^{-16}	23
AlGaAs	neat	1560		2×10^{-17}	23
PTS	neat	1600		1.5×10^{-16}	23
DAN	neat	630		5×10^{-16}	23
$MoOS_3Cu_2(PPh_3)_3$	7.4×10^{-5}	532	2.6×10^{-10}	5×10^{-17}	12
$Mo_2S_8Ag_4(PPh_3)_3$	1.3×10^{-4}	532	1.3×10^{-9}	1.6×10^{-16}	24
$MoOS_3(CuNCS)_3^{2-}$	6.1×10^{-3}	532	1.1×10^{-10}	-2.3×10^{-16}	10
$Mo_2O_2S_6Cu_6I_6^{4-}$	2×10^{-3}	532	4×10^{-10}	-6×10^{-17}	this work

important advantage in broad-band−low-loss photonic applications especially in the area of integrated optical circuits. (2) It has been noticed with certain third-order NLO organic chromophores that introduction of an inversion center at molecular level results in a decrease of the n_2/α_2 ratio of a molecule.[22] This tendency seems also present in other inorganic clusters studied (e.g rows 5 and 6 in Table 4). The underlying physics is not understood at this stage. A systematic study on the NLO properties of both the nest-shaped (acentric) and the twin-nest-shaped (centrosymmetric) clusters may shed light on this issue. It is obvious that more data needs to be accumulated before a sound relationship between chemical structures of inorganic clusters and their NLO properties can be well established.

Acknowledgment. The authors acknowledge support from Nanjing University, the Fujian Institute of Research on Structure of Matter, and the National University of Singapore.

Supporting Information Available: Tables of x-ray diffraction data collection and refinement procedures, cell parameters, atomic coordinates, bond distances, bond angles, and anisotropic displacement parameters, along with all of the corresponding estimated standard deviations, tables of least-squares planes, and corresponding dihedral angles and estimated standard deviations (12 pages). Ordering information is given on any current masthead page.

IC950991V

(22) Bahra, G. S., *Mater. Res. Soc. Symp. Proc.*, in press.
(23) Stegeman, G. I.; Torruellas, W., *Mater. Res. Soc. Symp. Proc.* **1994**, *328*, 397.
(24) Ji, W.; Shi, S.; Du, H. J.; Ge, P.; Tang, S. H.; Xin, X. Q. *J. Phys. Chem.* **1995**, *99*, 17297.